

1 **A bacterial prophage small peptide counteracts DnaA activities in *B.*** 2 ***subtilis*.**

3 **Magali Ventroux and Marie-Francoise Noirot-Gros***

4 Université Paris-Saclay, INRAE, AgroParisTech, Micalis Institute, 78350, Jouy-en-Josas, France.

5 *** Correspondence:**

6 marie-francoise.noirot-gros@inrae.fr

7 **Keywords:** small ORF, SEP, skin element, DnaA, Spo0A, *B. subtilis*

8

9 **Abstract**

10 Bacteriophages are able to hijack host essential machineries to benefit their fitness and assemble their
11 own progeny. Phage proteins targeting major bacterial pathways can be powerful tools to understand
12 cell functions and have possible applications in human health and industry. Bacterial genomes also
13 harbor cryptic prophages carrying genes that may contribute to their host fitness and properties. The
14 cryptic prophages are mostly transcriptionally silent and most of the functions they encode are not
15 annotated. In *B. subtilis*, the 48 kb-long *skin* element is a prophage carrying the *yqaF-yqaN* operon,
16 which is tightly regulated by the Xre-like repressor *sknR*. The small *yqaH* gene potentially encodes
17 the protein *YqaH* in absence of *SknR*. It was previously reported that *YqaH* interacts with the
18 replication initiator *DnaA* in yeast two-hybrid assay and its expression in *B. subtilis* causes defects in
19 the chromosomal cycle. In this study, we report that, in addition to *DnaA*, *YqaH* interacts with
20 *Spo0A*, a master regulator of sporulation. To decipher *yqaH* mode of action, we used the yeast two-
21 hybrid to isolate single mutations in *yqaH* that separate interactions with *DnaA* and *Spo0A*. We
22 isolated mutations that caused loss-of-interaction (LOI) with *DnaA* but not *Spo0A*. However, all
23 mutations disrupting the interaction with *Spo0A* were also *DnaA*-LOI functions, suggesting that
24 these functions could not be separated. We found that expression *YqaH* carrying *DnaA*-LOI
25 mutations affects both chromosome integrity and *DnaA*-mediated transcription, leading to growth
26 inhibition as well as preventing bacterial development such as sporulation and biofilm formation.
27 These results show that *YqaH* acts as an antimicrobial peptide in *B. subtilis* and pave the way for the
28 structural design of mutants with improved antibacterial action.

29

30 **1 Introduction**

31 Small proteins encoded by short open reading frames (smORFs) has emerged as a new class of
32 micropeptides widespread in both in eukaryotic and prokaryotic genomes (Albuquerque et al., 2015;
33 Couso and Patraquim, 2017; Hellens et al., 2016; Samayoa et al., 2011; Storz et al., 2014). Due to
34 their small size, smORFs have been overlooked for a long time. However, with advanced
35 computation and ribosome profiling-based biochemical methods, small proteins are being now more

36 widely identified and some has been functionally characterized (Chu et al., 2015; He et al., 2018;
37 Samayoa et al., 2011; Straub and Wenkel, 2017; VanOrsdel et al., 2018). Growing evidence indicates
38 they often encode bioactive peptides (Chu et al., 2015; Saghatelian and Couso, 2015). However, their
39 contribution to cellular functions remains largely unexplored.

40 Micropeptides (for the smallest <30aa or microProteins up to 100 aa) were identified to act as
41 regulators of diverse cellular processes in eukaryotes (Staudt and Wenkel, 2011). In plants,
42 characterized micro-proteins were found to regulate transcription factors by sequestering them into
43 nonfunctional states, preventing DNA binding or transcriptional activation (Dolde et al., 2018; Graeff
44 and Wenkel, 2012). In *Drosophila melanogaster*, smORF-encoded peptides (SEPs) represent about
45 5% of the transcriptome and play an important role in controlling drosophila development by
46 triggering post-translational processing of transcriptional regulators (Albuquerque et al., 2015; Zanet
47 et al., 2015). In human, SEPs has been discovered with specific subcellular localization, suggesting
48 they can fulfill biological functions (Slavoff et al., 2013). As example, a 69 aa long SEP, MRI-2,
49 has been described to play a role in stimulating DNA repair through binding to the DNA end-binding
50 protein complex Ku (Slavoff et al., 2014). SEPs represent about 2% of the genome of *S. cerevisiae*
51 (Erpf and Fraser, 2018). Their function remains largely elusive but few has been identified to play
52 regulatory roles in diverse physiological processes such as iron homeostasis (An et al., 2015) or DNA
53 synthetis (Chabes et al., 1999; Erpf and Fraser, 2018; Lee et al., 2008). Genomic analysis of the *S.*
54 *cerevisiae* sORFs revealed that a significant part are conserved in other eukaryotes even as
55 phylogenetically distantly related such as humans, thus emphasizing their biological significance
56 (Kastenmayer et al., 2006).

57 In Prokaryotes, small proteins are encoded by 10 to 20% of sRNA in average, and are often species-
58 specific (Friedman et al., 2017; Miravet-Verde et al., 2019; VanOrsdel et al., 2018; Yang et al., 2016;
59 Zuber, 2001). SEPs with characterized functions were found involved in various cellular processes
60 (Storz et al., 2014). In *P. aeruginosa*, PtrA (63-aa long) and PtrB (59-aa long) repress the type III
61 secretion system in response to DNA stress (Ha et al., 2004; Wu and Jin, 2005). In *E. coli*, the 43-aa
62 long peptide SrgT interferes with the PTS glucose transport system allowing cells to utilize
63 alternative non-PTS carbon sources to rapidly adapt to environmental changes in nutrient availability
64 (Lloyd et al., 2017). In *B. subtilis*, SEPs have been found to participate in regulating cell division and
65 stress responses (Ebmeier et al., 2012; Handler et al., 2008; Schmalisch et al., 2010). A compelling
66 example is the recently characterized developmental regulator MciZ (mother cell inhibitor of FtsZ), a
67 40-aa long peptide which prevents cytokinesis in the mother cell during sporulation (Araujo-Bazan et
68 al., 2019; Bisson-Filho et al., 2015). In this bacteria, about 20% of the total core protein of the mature
69 spores is composed by the small acid-soluble spore proteins (SASPs) playing an important role in
70 protecting DNA in the dormant spores (Moeller et al., 2008; Setlow, 2007). Notably, several
71 smORFs identified in intergenic regions were reported to be expressed during sporulation
72 (Schmalisch et al., 2010). The sporulation inhibitor *sda* encodes a 52aa long protein, which acts as a
73 checkpoint system coordinating DNA replication with sporulation initiation (Burkholder et al., 2001;
74 Cunningham and Burkholder, 2009; Rowland et al., 2004). Its mode of action has been extensively
75 characterized at molecular level. Sda binds to the primary sporulation kinase KinA, preventing its
76 activation and subsequent phosphorelay-mediated activation of the master sporulation regulator

77 Spo0A (Cunningham and Burkholder, 2009; Veening et al., 2009). By linking DNA replication to a
78 phosphorylation-dependent signaling cascade that triggers cellular development, this system
79 illustrates an important biological role played by a SEP in blocking sporulation in response to DNA
80 stress in *bacillus* (Veening et al., 2009).

81 Small proteins encoded by phage or by prophage-like regions of bacterial genomes have been
82 identified to hijack the host cellular machineries, as part of a strategy to shift host resources toward
83 the production of viral progeny (Liu et al., 2014; Duval and Cossart, 2017). The bacteriophage T7
84 gene 2 encodes the 64 aa-long gp2 protein essential for infection of *E. coli*. Studies of its biological
85 role revealed that gp2 inhibits transcription by binding to RNA polymerase (RNAP), promoting a
86 host-to-viral RNAP switch (Nechaev and Severinov, 2003; Savalia et al., 2010). Another illustration
87 is the 52-aa long protein ORF104 of phage 77 infecting *S. aureus*. ORF104 is able to interfere with
88 the host chromosome replication by binding to the ATPase domain of the helicase loader protein
89 DnaI, thus preventing the loading of the DNA helicase DnaC (Liu et al., 2004; Hood and Berger,
90 2016).

91 DNA replication is an essential process in all living organisms. Owing to their essentiality, proteins
92 that compose the orisome and the replisome machineries are potential targets for the development of
93 antimicrobials. In bacteria, DNA replication is initiated by the conserved initiator protein DnaA that
94 assembles to the chromosomal replication origin to elicit local DNA strand opening (Hwang and
95 Kornberg, 1992; Leonard and Grimwade, 2011; Mott and Berger, 2007; Ozaki and Katayama, 2009).
96 This step triggers the coordinated assembly of the proteins that will further build a functional
97 replication fork, from the DNA helicase, unwinding the DNA duplex, to the many components of the
98 replisome that form the replication machinery (Messer, 2002). In addition to its initiator activity,
99 DnaA acts as a transcription factor repressing or activating genes (Messer and Weigel, 2003). The
100 activity of the initiator DnaA is tightly controlled to coordinate chromosomal replication initiation
101 with other cellular processes during the bacterial cell cycle (Katayama et al., 2010; Scholefield and
102 Murray, 2013). Part of this control is mediated by protein-protein interactions and involves various
103 protein regulators that bind DnaA and affect his activity (Felicori et al., 2016; Jameson and
104 Wilkinson, 2017; Katayama et al., 2017; Riber et al., 2016; Skarstad and Katayama, 2013). In *B.*
105 *subtilis*, four proteins SirA, Soj, DnaD and YabA have been identified to regulate DnaA activity or
106 its assembly at OriC through direct interaction (Bonilla and Grossman, 2012; Felicori et al., 2016;
107 Martin et al., 2019; Murray and Errington, 2008).

108 Phage SEPs targeting important functions in bacteria are regarded as promising antimicrobial
109 peptides, and ignited a strong interest in their identification and characterization (Hood and Berger,
110 2016; Liu et al., 2004). The phage-like element skin of *B. subtilis* encodes about 60 proteins. The
111 skin element is repressed under most physiological conditions (Nicolas et al., 2012), silenced by the
112 skin repressor SknR (Figure 1A) (Kimura et al., 2010). Excision of skin from the genome restore
113 the integrity of sigK gene encoding the late sporulation σ K factor (Kunkel et al., 1990). Among the
114 skin ORFs, *yqaH* encodes the 85 aa-long polypeptide YqaH that has been previously identified to
115 bind to the replication initiator protein DnaA in a yeast two-hybrid genomic screen (Noirot-Gros et
116 al., 2002; Marchadier et al., 2011). When *yqaH* is overexpressed, bacillus cells exhibits aberrant

117 nucleoid morphological defects suggestive of replication deficiency (Kimura et al., 2010). In this
118 study, we further characterized the function of *yqaH* in antagonizing DnaA. In addition, we found
119 that YqaH also interacts with the master regulator Spo0A involved in developmental transitions to
120 sporulation and biofilm formation (Dubnau et al., 2016). As DnaA, Spo0A is a DNA-binding protein,
121 which, under its activated phosphorylated form (Spo0A-P) controls the expression of numerous
122 genes during the early stages of sporulation (Molle et al., 2003). To further understand the biological
123 role of this sORF in *B. subtilis* we performed the functional dissection of YqaH. Using a reverse
124 yeast two-hybrid system, we selected *yqaH* alleles that selectively disrupted the YqaH/DnaA
125 complex. This approach allowed us to link specific DnaA loss-of-interaction with loss-of-function
126 phenotypes

127

128 **2 Material and Methods**

129 **2.1 Strains, plasmids and primers**

130 Experiments were performed in strains 168 *trp*⁺ or TF8A a phage-cured strain lacking the prophage-
131 like element ‘skin’ element as well as the prophages SP β and PBSX (Nicolas et al., 2012; Westers et
132 al., 2003) (Table S1A). *Saccharomyces cerevisiae* PJ69-4a or α strains used for yeast-two-hybrid
133 experiments (James et al., 1996). *Escherichia coli* strain DH10B (Durfee et al., 2008) was used as a
134 cloning host. Plasmids constructs are listed in Table S1B. Primers are listed in Table S2. Sequences
135 of interest cloned or mutated in this study were verified by DNA sequencing.

136 **2.2 Bacterial culture conditions**

137 Bacteria strains were grown at 37°C in LB medium containing ampicillin 100 μ g/ml for plasmid
138 selection (in *E. coli*), spectinomycin 60 μ g/ml, kanamycin 5 μ g/ml or chloramphenicol 5 μ g/ml (for
139 *B. subtilis*), and inducer molecules IPTG 0.5 mM, or D-xylose 0.5%, when necessary. *B. subtilis*
140 strains containing pDG148 and pDG148-*yqaH* constructions were grown overnight in LB
141 complemented with kanamycin. ON cultures were then diluted at OD₆₀₀ 0.01 on fresh media and
142 grown to mid-exponential phase (OD₆₀₀ 0.3-0.4) prior to addition of IPTG. The effect of *yqaH*
143 expressing on growth has been performed in 96 microwells plates in a final volume of 200 μ L.

144 **2.3 Strains constructions**

145 *yqaH* expression:

146 The *yqaH* wild type and mutated gene derivatives, were PCR-amplified using the *yqaH-HindIII-RBS-*
147 *F/pYqaH-R* primer pair and inserted in plasmid pDG148 between HindIII and SalI restriction sites to
148 be placed under control of the IPTG-inducible *Pspac* promoter (Stragier et al., 1988). The plasmid
149 constructs were extracted from *E. coli* and transformed in *B. subtilis*. Expression of YqaH wild-type
150 and mutated proteins were assessed using 3xflag-fusions.

151 *Construction of yqaH-gfp fusion:*

152 *yqaH* WT and mutated gene were PCR-amplified from the pGAD-*yqaH* yeast vector derivatives
153 carrying either the WT or LOI mutations (see below) using *yqaH-apa* and *pYqaH-R* primer pair.
154 DNA fragments were digested by *ApaI* and *SalI* and inserted in between *ApaI* and *XhoI* restriction
155 sites of pSG1154m, a version of the pSG1154 vector (Lewis and Marston, 1999) encoding a
156 monomeric version of the GFP (GFPm). Final constructions, consisting of translational fusions of
157 the *gfpm* gene to the C-terminal region encoded *yqaH* under the control of the *P_{xyl}* promoter, were
158 transferred at the *amyE* locus of the *B. subtilis* chromosome by transforming competent *B. subtilis*
159 cells with plasmid DNA. The transfer of single mutations in the *spo0A* chromosomal locus of *B.*
160 *subtilis* were performed by gene replacement using the “pop-in pop-out” gene replacement method
161 (Fabret et al., 2002; Tanaka et al., 2013).

162

163 *Yeast two-hybrid plasmid constructs:*

164 Genes encoding for full size YqaH, Spo0A, YabA and DnaA, as well as truncated DnaA (boundaries
165 as illustrated figure 1D) were translationally fused to the activating domain (AD) or the binding
166 domain (BD) of the transcriptional factor Gal4 by cloning into pGAD and pGBDU vectors,
167 respectively (James et al., 1996). DNA fragments were amplified by PCR using appropriated primer
168 sets (Table S2), double digested by *EcoR1* and *SalI* and ligated to corresponding pGAD or pGBDU
169 linearized vector to generate a translational fusion with Gal4-AD or BD domains. Plasmid constructs
170 were first transformed into *E. coli* prior to be introduced pJ69-4 α (pGAD-derivatives) or pJ69-4a
171 (pGBDU-derivatives) haploid strain. pGAD- and pGBDU- plasmid derivatives were selected onto
172 SD media lacking leucine (SD-L) or Uracyl (SD-U), respectively (James et al., 1996).

173

174 **2.4 Sporulation conditions**

175 Sporulation of *B. subtilis* was induced by nutrient limitation by the re-suspension in Sterlini-
176 Mandelstam medium (SM) (Sterlini and Mandelstam, 1969). The beginning of sporulation (t_0) is
177 arbitrarily defined as the moment of re-suspension of the cells in SM. To study the effects of *yqaH*
178 overexpression on *B. subtilis* sporulation, ON cultures of strains containing the pDG148
179 constructions were then diluted in CH medium at starting OD600 of 0.05. When cultures reached an
180 OD600=1, cells were re-suspended in an equivalent volume of SM medium complemented with
181 0.5M IPTG (t_0). To monitored sporulation efficiency, cells were collected at different times after
182 sporulation induction (t_0) until t_6 (6 hours after induction, defined as a stage of production of mature
183 spores) and t_{18} . Asymmetric septa and spores were enumerated by microscopic observations from all
184 samples.

185 **2.5 Spores survival assay**

186 Cells were spread and grown ON at 30°C on DSM agar medium (Schaeffer et al., 1965), prior to be
187 inoculated in preheated liquid DSM at OD600 0.1 and incubated at 37°C until reaching OD600 1.5.
188 From this point (taken as T_0) cultures were grown for 20 h to produce matured resistant spores.
189 Samples were collected and half of the material was heated at 80°C (10 min) before plating to kill
190 potential vegetative cells prior to be plated on LB. Colony counts were performed after 36 hours at

191 37°C. The percentage of spores was calculated as the ratio of colonies forming units (cfu) from
192 heated and unheated samples.

193 **2.6 Yeast-two-hybrid assay**

194 The yeast-two-hybrid assays were performed as described (Marchadier et al., 2011; Noirot-Gros et
195 al., 2002; Noirot-Gros et al., 2006). PJ69-4A and α haploid yeast strains transformed by pGAD- and
196 pGBDU- plasmid derivatives were mixed onto YPD-rich media plates to allow formation of diploids.
197 Diploids containing both pGAD and pGBDU type of plasmids were then selected on SD-UL and
198 interacting phenotypes were monitored by the ability of diploids to grow on SD-LUHA medium
199 further lacking histidine (H) or adenine (A).

200 **2.7 Generation of Loss of Interaction (LOI) mutation**

201 YqaH_LOI mutants were identified using a yeast two-hybrid-based assay as described elsewhere
202 (Natrajan et al., 2009; Noirot-Gros et al., 2006; Quevillon-Cheruel et al., 2012). Random mutagenesis
203 of the targeted genes were achieved by PCR amplification under mutagenic conditions that promotes
204 less than one miss incorporation per amplification cycle (Noirot-Gros et al., 2006). For *yqaH*, a
205 library of mutated pGAD-*yqaH** were constructed by gap-repair recombination into yeast (PJ69-4 α
206 strain). About 1000 individual transformants were organized in 96-well format on plates containing a
207 defined medium lacking leucine (-L) to form an arrayed collection of AD-*yqaH** gene fusion
208 mutants. This organized library was then mated with PJ69-4a strains containing either pGBDU-
209 *dnaA* or pGBDU-*spo0A*, or an empty pGBDU plasmid as a negative control. Selective pressure for
210 interacting phenotypes was then applied on media lacking -LUH or -LUA. Diploids that failed to
211 grow on interaction selective media are considered as potentially expressing a loss-of-interaction
212 (LOI) mutant of *yqaH*. Importantly, any particular AD-YqaH*_LOI proteins unable to trigger
213 interacting phenotypes in the presence of BD-DnaA while still producing interacting phenotypes
214 when expressed in the presence of BD-Spo0A is defined as a DnaA-specific LOI mutant. The
215 corresponding *yqaH_LOI* genes were retrieved from the initially organized haploid library and the
216 mutations identified by DNA sequencing. Only mutations resulting from single substitutions were
217 considered.

218 **2.8 Ori/Ter ratios measurements by qPCR**

219 To determine the ratio of amounts of origin-proximal and terminus-proximal DNA sequences, ON
220 cultures of *B. subtilis* strains containing pDG148 or pDG148-*yqaH* plasmids were freshly diluted
221 (OD₆₀₀=0.01) in LB supplemented with kanamycin 5 μ g/mL in the presence of IPTG 0.5 mM, and
222 grown at 37°C in up to mid-exponential phase (OD₆₀₀ = 0.3 to 0.4). A determined volume of culture
223 was taken, mixed with similar volume of sodium azide solution (1%, 0.5% final) to stop all metabolic
224 activities, and subjected to total lysis. Total genomic DNA extracts were kept at -80°C and thawed
225 aliquots were used only once. Quantitative real time PCR were performed on a Mastercycler® ep
226 realplex (Eppendorf) thermocycler device using ABsolute™ Blue QPCR SYBR® Green ROX Mix
227 (ABgene), to amplify specific origin or terminus proximal sequences. Primers used for sequence
228 amplification were chosen using Primer3Plus program (<http://www.bioinformatics.nl/cgi->

229 [bin/primer3plus/primer3plus.cgi/](http://www.bioinformatics.nl/cgi-bin/primer3plus/primer3plus.cgi/)). Amplification using the ORI pair of primers (oriL3F and oriL3R,
230 Table S2) targeting the 4212889-4211510 region of the *B. subtilis* chromosome, yields a 128 bp size
231 product corresponding to sequence at the left side of the origin. The terminus sequence is a 122 bp
232 long fragment obtained from the TER pair of primers (terR3F and terR3R, Table S2) amplifying the
233 region 2016845-2017711 at the right side of the terminus. The two primer pairs ORI and TER
234 exhibited $\geq 95\%$ of amplification efficiency. Data analysis was performed using the software
235 Realplex (Eppendorf) and the quantification with the $\Delta\Delta C_t$ method. The formula reflects the efficacy
236 (Eff) of the primers ($\text{Rate} = (1 + \text{Eff})^{(-\Delta\Delta C_t)}$).

237

238 **2.9 Gene expression quantifications**

239 To quantify the expression rates of genes regulated by DnaA, sample of cells (as collected for Ori/Ter
240 ratios measurements) were also harvested in exponential growth at OD600=0.3-0.4, and RNA
241 extractions were performed. To quantify the expression rates of genes regulated by Spo0A,
242 sporulating cells were harvested when reaching stages T2-T3 of sporulation ($t_{2,5}$) in SM medium. In
243 both case, a determined volume of culture was mix with equivalent volume of centrifuged of sodium
244 azide solution, and subjected to lysis followed by total RNA extraction as described (Nicolas et al.,
245 2012). Total RNA was reversely transcribed and quantitative real time PCR were performed on
246 cDNA. Primers used for sequence amplification were chosen using Primer3Plus program
247 (<http://www.bioinformatics.nl/cgi-bin/primer3plus/primer3plus.cgi/>) and are detailed in Table S2.
248 The couples of primers exhibited $\geq 95\%$ amplification efficiency. Data analysis was performed using
249 the software Realplex (Eppendorf) and the quantification with the $\Delta\Delta C_t$ method. The formula reflects
250 the efficacy (Eff) of the primers ($\text{Rate} = (1 + \text{Eff})^{(-\Delta\Delta C_t)}$).

251

252 **2.10 Fluorescence microscopy**

253 The cytolocalization of proteins fused to GFP were observed by epifluorescence microscopy on
254 vegetative or sporulating cells. The expression of *yqaH-gfp* gene fusions from the *B. subtilis amyE*
255 chromosomal locus was triggered by supplementing exponential growth or sporulation cultures with
256 xylose 0.5%. Sample of cells were harvested and rinsed in a minimal transparent media to avoid LB
257 auto-fluorescence prior to be mounted onto 1.2% agarose pads. When necessary, bacterial
258 membranes were stained with FM4-64 dye and nucleoids with DAPI. Fluorescence microscopy was
259 performed on a Leica® DMR2A (100X UplanAPO objective with an aperture of 1.35.) coupled with
260 CoolSnap HQ camera (Roper Scientific). System control and image processing were achieved using
261 Metamorph software (Molecular Devices, Sunnyvale, CA, USA). Counts of cells, spores, foci or
262 nucleoids were determined with the ImageJ® software, from at least 500 cells.

263 **2.11 Biofilm assay**

264 Production and analysis of air-to-liquid biofilm pellicles were performed as already described (Garcia
265 Garcia et al., 2018). Briefly, strains expressing *yqaH*, wild type or K17E mutant derivative as well as
266 control strain were grown in LB to OD600 of 1.0 and inoculated in 12-well culture plates containing

267 3.5 ml of MSgg media at starting OD₆₀₀ = 0.1. Cultures were maintained at 28°C and 70% humidity,
268 with no agitation. After 48 hours, wells were filled out with MSgg media (slowly added at the edge)
269 to lift the biofilm pellicles up to the top of the wells. The pellicles were then peeled-off onto a 2.5 cm
270 diameter circular cover slide. The cover slides with intact biofilm pellicles were mounted onto an
271 Attofluor Cell Chamber and stained with the Film Tracer FM 1-43 Green Biofilm dye (Thermo
272 Fisher Scientific). Stained biofilms were observed using a spinning disk confocal microscope [Nikon
273 Eclipse Ti-E coupled with CREST X-Light™ confocal imager; objectives Nikon CFI Plan Fluor
274 10X, DIC, 10x/0.3 NA (WD = 16 mm); excitation was performed at 470 nm and emission recorded
275 at 505 nm]. Images were processed using IMARIS software (Bitplane, South Windsor, CT, United
276 States). Biofilm images were quantified using the surface function in IMARIS (XTension biofilm).
277 Biovolumes were calculated based on total volume (μm³) per area (μm²) from n ≥ 4 samples.

278 **2.12 Protein immunodetection**

279 Production of 3FLAG-YqaH mutated derivatives was determined from total protein extract of *B.*
280 *subtilis* by immuno-detection using monoclonal antibody anti-FLAG[®] M2 (Sigma). An IgG goat
281 secondary antibody (Sigma) peroxidase conjugated was used at 1/10000e to detect the anti-FLAG[®]
282 M2. Proteins immuno-detections were performed using the Clarity Western ECL kit (Biorad)
283 according to the supplier's indications followed by chemiluminescence detection (ChemiDoc imager,
284 Biorad). Images were analysed with the software Image Lab™.

285 **2.13 Structure predictions**

286 Secondary structures predictions were performed with the computer server Jpred 3
287 (<http://www.compbio.dundee.ac.uk/www-jpred/>) and 3D structures predictions with the server Phyre²
288 (<http://www.sbg.bio.ic.ac.uk/phyre2/html/page.cgi?id=index>).

289

290 **3 Results**

291 **3.1 The Skin element SPORF YqaH interacts with DnaA and Spo0A**

292 YqaH was originally identified as interacting with the replication initiator DnaA in a yeast two-
293 hybrid screen of a *B. subtilis* genomic library (Noirot-Gros et al., 2002). Interestingly, we also
294 identified YqaH as binding partner to Spo0A in a subsequent screen targeting the sporulation
295 transcriptional factor (Figure 1B). Other DnaA-binding proteins SirA, Soj, DnaD and YabA also
296 exert regulatory functions by interacting with different functional domains of DnaA (Figure 1B). To
297 gain insights into YqaH mode of action, we characterized the minimal interacting domain of DnaA.
298 We defined the C-terminal domain IV as necessary and sufficient to trigger the interaction
299 phenotypes in a yeast two-hybrid binary assay (Figure 1C). This 118 AA long fragment spans residue
300 328 to 446, and carries the signature motif for binding to double stranded DNA. This result
301 distinguishes YqaH from other regulators, found to inhibit DnaA binding to *oriC* through interacting
302 with domains I, responsible for self-oligomerization (SirA), and/or the central AAA+ ATPase
303 domain III, (SirA, Soj, YabA and DnaD).

304 **3.2 YqaH expression triggers *dnaA*-related mutant phenotypes**

305 The interaction of YqaH with DnaA hints at a potential role in replication initiation control. We first
306 investigated the effect of *yqaH* expression on cell growth and viability. *B. subtilis* strains carrying a
307 plasmid expressing *yqaH* under control of an IPTG-inducible promoter or carrying a control plasmid
308 with no expressed gene were treated under identical conditions. Addition of IPTG at early exponential
309 stage specifically halted cell growth after two hours in cells expressing *yqaH* (Figure 2A). We found
310 that cell viability was affected almost instantly in the presence of *yqaH*, leading to about 30x
311 decrease after three hours (Figure 2A). Expression of *yqaH* also affects cell morphology leading to
312 significant filamentation (Figure 2B). Closer examination of nucleoids revealed aberrant segregation
313 of chromosomes with both diffused and compacted nucleoids unequally distributed within filaments,
314 as well as a large portion of cells with no DNA. Most importantly, septum-entrapped nucleoids were
315 also observed indicative of impaired nucleoid occlusion (NO) (Wu and Errington, 2011). These
316 observations highlighted that the expression of YqaH triggered a large panel of chromosomal
317 disorders suggestive of replication and segregation stress, and compatible with replication initiation
318 deficiency, in agreement to earlier described (Kimura et al., 2010). We further investigate a role of
319 YqaH by investigating DnaA-dependant transcriptional regulation. Among genes of the DnaA-
320 regulon, active DnaA-ATP negatively regulate its own expression by binding to *dnaA* promoter
321 region (Goranov et al., 2005). We monitored the *dnaA* mRNA levels in the presence or absence of
322 YqaH and shown that expression of *yqaH* led to a 2 fold increase in *dnaA* mRNA, indicating a
323 regulatory defect. Taking all together, these results are in agreement with a direct role of YqaH in
324 counteracting DnaA activity.

326 **3.3 YqaH expression impairs sporulation**

327 We investigated the possible role of YqaH in Spo0A functions, by examining the effect of *yqaH*
328 expression on sporulation. Cells carrying either the control or the *yqaH*-inducible plasmids were put
329 to sporulate by the re-suspension method. To prevent an inhibitory effect of YqaH during vegetative
330 growth, the *yqaH* gene expression was induced only at the onset of sporulation (T0). The formation
331 of spores was monitored over time. Appearance of asymmetric septa at early stage (T2,5) was imaged
332 by fluorescent microscopy after staining by a red-fluorescent membrane-dye, while the engulfed
333 forespore (T6 and T18) was revealed using bright field (Figure. 3A). We observed that the counts of
334 spore forming bacteria was drastically affected in the presence of YqaH (Figure 3B). We also
335 examined the effect of *yqaH* expression on Spo0A-mediated transcriptional regulation. Among the
336 genes under the direct control of Spo0A are *spoIIIE*, encoding the protein serine phosphatase SpoIIIE
337 and *spoIIIGA*, encoding a pro- σ E processing protease (Molle et al., 2003). These two genes are
338 involved in the activation of the alternative sporulation sigma factors σ F and σ E in the forespore and
339 mother cell compartments, respectively (Baldus et al., 1994; Bradshaw et al., 2017; Errington and
340 Wu, 2017; Fujita et al., 2005). Examination of their expression at the onset of sporulation revealed a
341 significant downregulation (about 7 and 8 fold, respectively) in the presence of *yqaH* (Figure 3C).
342 Altogether, these results pointed to a negative effect of YqaH in Spo0A-mediated function.

343

344 **3.4 Functional dissection of YqaH**

345 To further decipher YqaH mechanism, we looked for *yqaH* separation of function mutations that
346 selectively affect its ability to interact to one protein partner while preserving its interaction with the
347 other. Using a yeast two-hybrid based assay, we screened a *yqaH* mutant library specific loss-of-
348 interaction (LOI) phenotypes (Figure S1A). This approach is based on the selection of single
349 amino acid changes in the protein of interest that selectively disrupt the interaction with one partner
350 without affecting the interaction with the other partner. Such screening favors the substitution of
351 residues located at the interacting surface, leading to a LOI phenotype with the targeted partner,
352 while preserving the overall 3D-structure of the protein that remains proficient for interaction with
353 another partner (Natrajan et al., 2009; Noirot-Gros et al., 2006; Quevillon-Cheruel et al., 2012). We
354 identify three single residue substitutions K17E, E38K and K48E that elicited a complete loss-of-
355 interaction phenotype with DnaA without affecting interaction with Spo0A (Figure S1B, Table 1).
356 Six additional substitutions affecting residues R16G, M27T, Y37H, E38V A44V and R56W were
357 only partially abolishing interaction phenotypes with DnaA (Figure S1B, Table 1). Two substitutions,
358 S25T and A40T were found to partially affect both interaction with DnaA and Spo0A, and 4
359 substitutions, D10G, S20L, L28P, L43P and L57P were totally abolishing interaction phenotypes
360 with both DnaA and Spo0A (Figure S1B, Table1). In the latter case, these substitutions could have
361 affected the overall YqaH 3D-structure integrity. Is it worthy of note that, while several specific
362 DnaA-LOI mutants were obtained, no substitution that specifically prevent interaction with Spo0A
363 were identified in our screen. The YqaH protein is predicted to fold into three successive alpha helix
364 (Figure S1B). The residues important for interaction with DnaA mapped within the two main helix
365 presumably involved in a coiled-coil structure.

366

367 **3.5 DnaA-LOI mutants of *yqaH* restore replication and transcriptional regulation defects** 368 **caused by YqaH expression**

369 We investigated the effect of two DnaA-LOI mutants carrying substitutions K17E and R56W,
370 exhibiting total (K17E) or partial (R56W) loss of interaction phenotypes with YqaH in our yeast two-
371 hybride assay. (Table 1). Both substitutions abolished the nucleoid segregation defects resulting from
372 *yqaH* expression (Figure 4A). To rule out that this phenotypic compensation could potentially result
373 from expression of the gene copy from the silent *SknR* operon, we confirmed that the only source of
374 YqaH in the cell arisen from plasmidic expression (Figure S3). No YqaH protein was detected in
375 cells carrying a control plasmid devoid of *yqaH* coding sequence, indicating that the chromosomal
376 copy remained completely silent during our experimental conditions.

377 We further examined the effect of YqaH on replication initiation by measuring the ratio between
378 chromosomal origin-proximal and terminus-proximal sequences (Figure 4B). The average of origin-
379 to-terminus (*ori:ter*) ratio was determined by qPCR on genomic DNA harvested from exponentially
380 growing cells as previously described (Soufo et al., 2008). The *ori:ter* ratio was about 4 in control
381 cells that do not expressed *yqaH*, indicating that two events of replication initiation has taken place in
382 most cells, in agreement to already observed in similar experimental conditions (Murray and Koh,
383 2014). In the presence of *yqaH*, the *ori:ter* ratio dropped to 2, indicating that only one replication

384 initiation event per cell has taken place in average (Figure 4B). This observation suggests that the
385 YqaH protein could exerts a negative effect on replication initiation by counteracting DnaA activity.
386 We observed that this effect was abolished upon expression of the *yqaH*_DnaA LOI variants carrying
387 either the K17E or the R56W substitutions (Figure 4B). In cells, expressing YqaH-R56W the
388 replication initiation rate was similar to control cells while expression of YqaH-K17E restored about
389 75% of the initiation rate indicating a significant but partial complementation. In another assay, we
390 analyzed the number of chromosomal origin in individual cells using the *lacO*/LacI-GFP system.
391 Cells carrying a *lacO* repeat array near the replication origin and expressing the LacI-GFP fusion
392 were observed by fluorescence microscopy, in the presence of absence of YqaH (Figure 4C). In the
393 absence of YqaH, the number of lacI foci per nucleoid was found to be 3.6 in average, in agreement
394 with the *ori-to-ter* ratio (Figure 4D). This number dropped to 1 upon expression of YqaH, suggestive
395 of replication deficiency. As observed earlier, cell were also exhibiting aberrant nucleoids and
396 segregation defects. Conversely, expression of YqaH-K17E mutant fully restored nucleoid and cell
397 morphology and partially restored replication defects with an average of LacI-GFP foci about 2.3.
398 Together these observations indicate that YqaH binds to DnaA and antagonized its activity in
399 replication initiation.

400 To substantiate the role of YqaH/ DnaA interaction, we also examined the effect of the DnaA-LOI
401 mutant on *dnaA* transcription (Figure 4E). We found that the loss of DnaA-mediated control of *dnaA*
402 expression in the presence of wild type YqaH was restored by the introduction of both K17E and
403 R56W substitutions. This result further supports the conclusion that the binding of YqaH to DnaA
404 antagonizes DnaA functions.

405

406 **3.6 The YqaH-mediated defects in sporulation and biofilm formation requires interaction** 407 **with DnaA.**

408 Although we did not identified any YqaH_SpoA-LOI mutant in our screen, we thought that the
409 YqaH_K17E DnaA-LOI mutant provided for a convenient separation-of-function for a more reliable
410 investigation of the potential role of *yqaH* in *spo0A*-mediated phenotypes. Indeed, this K17E variant
411 remains fully proficient for interacting with Spo0A in our yeast 2HB assays, allowing to investigate
412 the role of *yqaH* during sporulation while circumventing DnaA-related defects during vegetative
413 cycle. We compared the sporulation efficiencies of strains expressing the wild-type YqaH or the
414 YqaH_K17E variant in both 168 and TF8A (devoid of Skin element) backgrounds. The percent of
415 cells ongoing sporulation was determined at t6 (i.e stage VI, refers as the spore maturation stage,
416 Figure 5A). Surprisingly, we found that the K17E-LOI substitution abolished the defect elicited by
417 the wild type YqaH (Figure 5). This observation indicates that the sporulation deficiency mediated by
418 YqaH requires its ability to interact with DnaA. To further investigate the potential role of YqaH in
419 Spo0A-related processes, we also examined its effect on biofilm formation (Figure 5B, Figure S4).
420 We observed that the production of biofilm pellicles at the air-medium interface was impaired in
421 strains expressing YqaH, leading to a loss of biomass and cohesion. Damaged biofilm pellicles were
422 not observed in cells expressing the YqaH_K17E DnaA-LOI mutant (Figure 5B, Figure S4B,C) thus
423 pointing to a role of DnaA during biofilm formation.

424 **4 Discussion**

425 Our study sheds light on the mechanism of action of YqaH, a small protein with antimicrobial
426 activities encoded by the *B. subtilis* skin element. By physically interacting with two master
427 regulators DnaA and Spo0A, the YqaH protein holds the promise to inhibit two essential cellular
428 processes under two different life styles of the bacteria. Upon nutrient stress and other environmental
429 conditions, *B. subtilis* cells switch from vegetative growth to sporulation or biofilm formation. DnaA
430 is essential during vegetative growth, acting as both replication initiator and transcriptional factor,
431 while the response regulator Spo0A controls developmental transitions.

432 In *Bacillus*, several regulatory proteins inhibit DnaA by targeting different functional domains of the
433 protein. In cells committed to sporulation, the protein SirA prevents DnaA from binding to the
434 replication origin OriC by interacting with its structural domains I and III (Jameson et al., 2014).
435 During vegetative growth, the regulatory proteins YabA interacts with DnaA during most of the cell
436 cycle (Felicori et al., 2016; Noiro-Gros et al., 2006; Soufo et al., 2008). YabA as well as the
437 primosomal protein DnaD affect DnaA cooperative binding to OriC by interacting with DnaA
438 structural domain III (Merrikh and Grossman, 2011; Scholefield and Murray, 2013). Finally, the
439 ATPase protein Soj negatively regulates DnaA by also interacting with the structural domain III,
440 preventing oligomerization (Scholefield et al., 2011). Our results indicate that YqaH controls DnaA
441 activity by a mode distinct from the other known regulators, specifically by contacting the structural
442 domain IV of DnaA that is responsible for DnaA-box sequence recognition (Fujikawa et al., 2003).

443 *B. subtilis* cells expressing YqaH exhibited various DnaA-related phenotypes that spanned from a
444 general growth defect, aberrant nucleoid morphology, impaired replication initiation and loss of
445 transcriptional control (Figure 2 and 4). These cells also exhibited Spo0A-related phenotypes such as
446 a dramatic reduction of sporulation efficiency (Figure 3A, B), an inhibition of the expression of
447 Spo0A-dependent genes (Figure 3C) and a strong impairment of biofilm formation (Figure 5). These
448 observations are in agreement with a role of YqaH in counteracting both DnaA and Spo0A activities
449 during vegetative growth and sporulation. However, it is well documented that initiation of
450 sporulation is closely coupled to the cell cycle and DNA replication in order to ensure that
451 sporulation occurs only in cells containing two fully replicated chromosomes (Veening et al., 2009).
452 Because of this intricate relationship between DNA replication and sporulation, it is difficult to
453 separate the phenotypes of YqaH related to its interactions with DnaA on one hand and Spo0A on the
454 other hand. By using YqaH single point mutants unable to interact with DnaA while remaining
455 proficient for interaction with Spo0A, we identified mutational pattern on YqaH (Figure S2) and
456 demonstrated their direct involvement in DnaA-related a loss-of-function phenotype. In our screens,
457 we did not obtain YqaH mutants that affected only the interaction with Spo0A. However, the YqaH
458 DnaA_LOI mutants revealed that sporulation and biofilm formation phenotypes of YqaH expression
459 required interaction with DnaA. Thus, we could not establish whether interaction with Spo0A plays a
460 role in these phenotypes. Our results could be explained by the role of DnaA as a pleiotropic
461 transcriptional regulator controlling the expression of several sporulation genes, including the
462 checkpoint histidine kinase Sda (Washington et al., 2017). Sda is known to bind to KinA, inhibiting
463 its phosphorylation activity required to activate Spo0A (Burkholder et al., 2001). A recent study

464 highlighted that a large part of the role of DnaA into gene expression is indirect and mediated by sda
465 (Washington et al., 2017). Sda is positively regulated by both DnaA and Spo0A, and a coupling
466 between expression of Sda and the replication cycle results in cyclic bursts of Spo0A activation
467 (Narula et al., 2015). Many genes that appear regulated by DnaA are involved in sporulation and
468 biofilm formation, illustrating the complexity of regulatory circuits that control transitions in
469 lifestyle. In conclusion, our study characterizes the role of small peptide YqaH that negatively
470 interferes with a broad range of cellular processes by counteracting the activity of DnaA. Controlling
471 YqaH expression could be part of a strategy to prevent the dissemination of engineered *B. subtilis*
472 strains in a controlled environment.

473 **5 Acknowledgements**

474 **6 Author contributions**

475 MV and MFNG designed the experiments. MV performed all experiments. MV and MFNG
476 interpreted the results. MFNG wrote the manuscript. Both authors contributed to data interpretation
477 and reviewed the final version of the manuscript.

478 **7 Conflict of Interest**

479 The authors declare that the research was conducted in the absence of any commercial or financial
480 relationships that could be construed as a potential conflict of interest.

481 **8 Supplementary material**

482 Figure S1: Yeast 2HB screening of a yqaH gene mutant library for specific LOI phenotypes.

483 Figure S2: Mapping of the YqaH single LOI mutations with DnaA

484 Figure S3: Immunodetection of YqaH in cell extracts after induction

485 Figure S4: DnaA-dependant YqaH-mediated defects in biofilm formation

486 Figure S5: ORF conservation within bacillus species

487 Table S1: Strains and Plasmids

488 Table S2: Primers list

489

490 **9 References**

491 Albuquerque, J.P., Tobias-Santos, V., Rodrigues, A.C., Mury, F.B., and da Fonseca, R.N. (2015).
492 small ORFs: A new class of essential genes for development. *Genetics and molecular biology* 38,
493 278-283.

- 494 An, X., Zhang, C., Sclafani, R.A., Seligman, P., and Huang, M. (2015). The late-annotated small
495 ORF LSO1 is a target gene of the iron regulon of *Saccharomyces cerevisiae*. *MicrobiologyOpen* 4,
496 941-951.
- 497 Araujo-Bazan, L., Huecas, S., Valle, J., Andreu, D., and Andreu, J.M. (2019). Synthetic
498 developmental regulator MciZ targets FtsZ across *Bacillus* species and inhibits bacterial division.
499 *Mol Microbiol* 111, 965-980.
- 500 Baldus, J.M., Green, B.D., Youngman, P., and Moran, C.P., Jr. (1994). Phosphorylation of *Bacillus*
501 *subtilis* transcription factor Spo0A stimulates transcription from the spoIIG promoter by enhancing
502 binding to weak 0A boxes. *J Bacteriol* 176, 296-306.
- 503 Bisson-Filho, A.W., Discola, K.F., Castellen, P., Blasios, V., Martins, A., Sforca, M.L., Garcia, W.,
504 Zeri, A.C., Erickson, H.P., Dessen, A., *et al.* (2015). FtsZ filament capping by MciZ, a
505 developmental regulator of bacterial division. *Proc Natl Acad Sci U S A* 112, E2130-2138.
- 506 Bonilla, C.Y., and Grossman, A.D. (2012). The primosomal protein DnaD inhibits cooperative DNA
507 binding by the replication initiator DnaA in *Bacillus subtilis*. *J Bacteriol* 194, 5110-5117.
- 508 Bradshaw, N., Levdivikov, V.M., Zimanyi, C.M., Gaudet, R., Wilkinson, A.J., and Losick, R. (2017).
509 A widespread family of serine/threonine protein phosphatases shares a common regulatory switch
510 with proteasomal proteases. *Elife* 6.
- 511 Burkholder, W.F., Kurtser, I., and Grossman, A.D. (2001). Replication initiation proteins regulate a
512 developmental checkpoint in *Bacillus subtilis*. *Cell* 104, 269-279.
- 513 Chabes, A., Domkin, V., and Thelander, L. (1999). Yeast Sml1, a protein inhibitor of ribonucleotide
514 reductase. *J Biol Chem* 274, 36679-36683.
- 515 Chu, Q., Ma, J., and Saghatelian, A. (2015). Identification and characterization of sORF-encoded
516 polypeptides. *Crit Rev Biochem Mol Biol* 50, 134-141.
- 517 Couso, J.P., and Patraquim, P. (2017). Classification and function of small open reading frames.
518 *Nature reviews Molecular cell biology* 18, 575-589.
- 519 Cunningham, K.A., and Burkholder, W.F. (2009). The histidine kinase inhibitor Sda binds near the
520 site of autophosphorylation and may sterically hinder autophosphorylation and phosphotransfer to
521 Spo0F. *Mol Microbiol* 71, 659-677.
- 522 Dolde, U., Rodrigues, V., Straub, D., Bhati, K.K., Choi, S., Yang, S.W., and Wenkel, S. (2018).
523 Synthetic MicroProteins: Versatile Tools for Posttranslational Regulation of Target Proteins. *Plant*
524 *physiology* 176, 3136-3145.
- 525 Dubnau, E.J., Carabetta, V.J., Tanner, A.W., Miras, M., Diethmaier, C., and Dubnau, D. (2016). A
526 protein complex supports the production of Spo0A-P and plays additional roles for biofilms and the
527 K-state in *Bacillus subtilis*. *Mol Microbiol* 101, 606-624.
- 528 Durfee, T., Nelson, R., Baldwin, S., Plunkett, G., Burland, V., Mau, B., Petrosino, J.F., Qin, X.,
529 Muzny, D.M., Ayele, M., *et al.* (2008). The complete genome sequence of *Escherichia coli* DH10B:
530 Insights into the biology of a laboratory workhorse. *Journal of Bacteriology* 190, 2597-2606.
- 531 Ebmeier, S.E., Tan, I.S., Clapham, K.R., and Ramamurthi, K.S. (2012). Small proteins link coat and
532 cortex assembly during sporulation in *Bacillus subtilis*. *Mol Microbiol* 84, 682-696.
- 533 Erpf, P.E., and Fraser, J.A. (2018). The Long History of the Diverse Roles of Short ORFs: sPEPs in
534 Fungi. *Proteomics* 18, e1700219.

- 535 Errington, J., and Wu, L.J. (2017). Cell Cycle Machinery in *Bacillus subtilis*. Sub-cellular
536 biochemistry *84*, 67-101.
- 537 Fabret, C., Ehrlich, S.D., and Noirot, P. (2002). A new mutation delivery system for genome-scale
538 approaches in *Bacillus subtilis*. *Mol Microbiol* *46*, 25-36.
- 539 Felicori, L., Jameson, K.H., Roblin, P., Fogg, M.J., Garcia-Garcia, T., Ventroux, M., Cherrier, M.V.,
540 Bazin, A., Noirot, P., Wilkinson, A.J., *et al.* (2016). Tetramerization and interdomain flexibility of
541 the replication initiation controller YabA enables simultaneous binding to multiple partners. *Nucleic*
542 *Acids Res* *44*, 449-463.
- 543 Friedman, R.C., Kalkhof, S., Doppelt-Azeroual, O., Mueller, S.A., Chovancova, M., von Bergen, M.,
544 and Schwikowski, B. (2017). Common and phylogenetically widespread coding for peptides by
545 bacterial small RNAs. *BMC genomics* *18*, 553.
- 546 Fujita, M., Gonzalez-Pastor, J.E., and Losick, R. (2005). High- and low-threshold genes in the Spo0A
547 regulon of *Bacillus subtilis*. *J Bacteriol* *187*, 1357-1368.
- 548 Graeff, M., and Wenkel, S. (2012). Regulation of protein function by interfering protein species.
549 *Biomolecular concepts* *3*, 71-78.
- 550 Ha, U.H., Kim, J., Badrane, H., Jia, J., Baker, H.V., Wu, D., and Jin, S. (2004). An in vivo inducible
551 gene of *Pseudomonas aeruginosa* encodes an anti-ExsA to suppress the type III secretion system.
552 *Mol Microbiol* *54*, 307-320.
- 553 Handler, A.A., Lim, J.E., and Losick, R. (2008). Peptide inhibitor of cytokinesis during sporulation
554 in *Bacillus subtilis*. *Mol Microbiol* *68*, 588-599.
- 555 He, C., Jia, C., Zhang, Y., and Xu, P. (2018). Enrichment-Based Proteogenomics Identifies
556 Microproteins, Missing Proteins, and Novel smORFs in *Saccharomyces cerevisiae*. *J Proteome Res*
557 *17*, 2335-2344.
- 558 Hellens, R.P., Brown, C.M., Chisnall, M.A.W., Waterhouse, P.M., and Macknight, R.C. (2016). The
559 Emerging World of Small ORFs. *Trends in plant science* *21*, 317-328.
- 560 Hood, I.V., and Berger, J.M. (2016). Viral hijacking of a replicative helicase loader and its
561 implications for helicase loading control and phage replication. *Elife* *5*.
- 562 Hwang, D.S., and Kornberg, A. (1992). Opening of the replication origin of *Escherichia coli* by
563 DnaA protein with protein HU or IHF. *J Biol Chem* *267*, 23083-23086.
- 564 James, P., Halladay, J., and Craig, E.A. (1996). Genomic libraries and a host strain designed for
565 highly efficient two-hybrid selection in yeast. *Genetics* *144*, 1425-1436.
- 566 Jameson, K.H., and Wilkinson, A.J. (2017). Control of Initiation of DNA Replication in *Bacillus*
567 *subtilis* and *Escherichia coli*. *Genes* *8*.
- 568 Kastenmayer, J.P., Ni, L., Chu, A., Kitchen, L.E., Au, W.C., Yang, H., Carter, C.D., Wheeler, D.,
569 Davis, R.W., Boeke, J.D., *et al.* (2006). Functional genomics of genes with small open reading
570 frames (sORFs) in *S. cerevisiae*. *Genome research* *16*, 365-373.
- 571 Katayama, T., Kasho, K., and Kawakami, H. (2017). The DnaA Cycle in *Escherichia coli*:
572 Activation, Function and Inactivation of the Initiator Protein. *Front Microbiol* *8*, 2496.
- 573 Katayama, T., Ozaki, S., Keyamura, K., and Fujimitsu, K. (2010). Regulation of the replication
574 cycle: conserved and diverse regulatory systems for DnaA and oriC. *Nat Rev Microbiol* *8*, 163-170.

- 575 Kimura, T., Amaya, Y., Kobayashi, K., Ogasawara, N., and Sato, T. (2010). Repression of sigK
576 intervening (skin) element gene expression by the CI-like protein SknR and effect of SknR depletion
577 on growth of *Bacillus subtilis* cells. *J Bacteriol* *192*, 6209-6216.
- 578 Lee, Y.D., Wang, J., Stubbe, J., and Elledge, S.J. (2008). Dif1 is a DNA-damage-regulated facilitator
579 of nuclear import for ribonucleotide reductase. *Molecular cell* *32*, 70-80.
- 580 Leonard, A.C., and Grimwade, J.E. (2011). Regulation of DnaA assembly and activity: taking
581 directions from the genome. *Annual review of microbiology* *65*, 19-35.
- 582 Lewis, P.J., and Marston, A.L. (1999). GFP vectors for controlled expression and dual labelling of
583 protein fusions in *Bacillus subtilis*. *Gene* *227*, 101-110.
- 584 Liu, J., Dehbi, M., Moeck, G., Arhin, F., Bauda, P., Bergeron, D., Callejo, M., Ferretti, V., Ha, N.,
585 Kwan, T., *et al.* (2004). Antimicrobial drug discovery through bacteriophage genomics. *Nature*
586 *biotechnology* *22*, 185-191.
- 587 Lloyd, C.R., Park, S., Fei, J., and Vanderpool, C.K. (2017). The Small Protein SgrT Controls
588 Transport Activity of the Glucose-Specific Phosphotransferase System. *J Bacteriol* *199*.
- 589 Marchadier, E., Carballido-Lopez, R., Brinster, S., Fabret, C., Mervelet, P., Bessieres, P., Noirot-
590 Gros, M.F., Fromion, V., and Noirot, P. (2011). An expanded protein-protein interaction network in
591 *Bacillus subtilis* reveals a group of hubs: Exploration by an integrative approach. *Proteomics* *11*,
592 2981-2991.
- 593 Martin, E., Williams, H.E.L., Pitoulias, M., Stevens, D., Winterhalter, C., Craggs, T.D., Murray, H.,
594 Searle, M.S., and Soultanas, P. (2019). DNA replication initiation in *Bacillus subtilis*: structural and
595 functional characterization of the essential DnaA-DnaD interaction. *Nucleic Acids Res* *47*, 2101-
596 2112.
- 597 Messer, W. (2002). The bacterial replication initiator DnaA. DnaA and oriC, the bacterial mode to
598 initiate DNA replication. *FEMS microbiology reviews* *26*, 355-374.
- 599 Messer, W., and Weigel, C. (2003). DnaA as a transcription regulator. *Methods in enzymology* *370*,
600 338-349.
- 601 Miravet-Verde, S., Ferrar, T., Espadas-Garcia, G., Mazzolini, R., Gharrab, A., Sabido, E., Serrano,
602 L., and Lluch-Senar, M. (2019). Unraveling the hidden universe of small proteins in bacterial
603 genomes. *Molecular systems biology* *15*, e8290.
- 604 Moeller, R., Setlow, P., Horneck, G., Berger, T., Reitz, G., Rettberg, P., Doherty, A.J., Okayasu, R.,
605 and Nicholson, W.L. (2008). Roles of the major, small, acid-soluble spore proteins and spore-specific
606 and universal DNA repair mechanisms in resistance of *Bacillus subtilis* spores to ionizing radiation
607 from X rays and high-energy charged-particle bombardment. *J Bacteriol* *190*, 1134-1140.
- 608 Molle, V., Fujita, M., Jensen, S.T., Eichenberger, P., Gonzalez-Pastor, J.E., Liu, J.S., and Losick, R.
609 (2003). The Spo0A regulon of *Bacillus subtilis*. *Mol Microbiol* *50*, 1683-1701.
- 610 Mott, M.L., and Berger, J.M. (2007). DNA replication initiation: mechanisms and regulation in
611 bacteria. *Nat Rev Microbiol* *5*, 343-354.
- 612 Murray, H., and Errington, J. (2008). Dynamic control of the DNA replication initiation protein
613 DnaA by Soj/ParA. *Cell* *135*, 74-84.
- 614 Murray, H., and Koh, A. (2014). Multiple regulatory systems coordinate DNA replication with cell
615 growth in *Bacillus subtilis*. *PLoS Genet* *10*, e1004731.

- 616 Natrajan, G., Noirot-Gros, M.F., Zawilak-Pawlik, A., Kapp, U., and Terradot, L. (2009). The
617 structure of a DnaA/HobA complex from *Helicobacter pylori* provides insight into regulation of
618 DNA replication in bacteria. *Proc Natl Acad Sci U S A* *106*, 21115-21120.
- 619 Nicolas, P., Mader, U., Dervyn, E., Rochat, T., Leduc, A., Pigeonneau, N., Bidnenko, E., Marchadier,
620 E., Hoebeke, M., Aymerich, S., *et al.* (2012). Condition-dependent transcriptome reveals high-level
621 regulatory architecture in *Bacillus subtilis*. *Science* *335*, 1103-1106.
- 622 Noirot-Gros, M.F., Dervyn, E., Wu, L.J., Mervelet, P., Errington, J., Ehrlich, S.D., and Noirot, P.
623 (2002). An expanded view of bacterial DNA replication. *Proc Natl Acad Sci U S A* *99*, 8342-8347.
- 624 Noirot-Gros, M.F., Velten, M., Yoshimura, M., McGovern, S., Morimoto, T., Ehrlich, S.D.,
625 Ogasawara, N., Polard, P., and Noirot, P. (2006). Functional dissection of YabA, a negative regulator
626 of DNA replication initiation in *Bacillus subtilis*. *Proc Natl Acad Sci U S A* *103*, 2368-2373.
- 627 Ozaki, S., and Katayama, T. (2009). DnaA structure, function, and dynamics in the initiation at the
628 chromosomal origin. *Plasmid* *62*, 71-82.
- 629 Quevillon-Cheruel, S., Campo, N., Mirouze, N., Mortier-Barriere, I., Brooks, M.A., Boudes, M.,
630 Durand, D., Soulet, A.L., Lisboa, J., Noirot, P., *et al.* (2012). Structure-function analysis of
631 pneumococcal DprA protein reveals that dimerization is crucial for loading RecA recombinase onto
632 DNA during transformation. *Proc Natl Acad Sci U S A* *109*, E2466-2475.
- 633 Riber, L., Frimodt-Moller, J., Charbon, G., and Lobner-Olesen, A. (2016). Multiple DNA Binding
634 Proteins Contribute to Timing of Chromosome Replication in *E. coli*. *Frontiers in molecular*
635 *biosciences* *3*, 29.
- 636 Rowland, S.L., Burkholder, W.F., Cunningham, K.A., Maciejewski, M.W., Grossman, A.D., and
637 King, G.F. (2004). Structure and mechanism of action of Sda, an inhibitor of the histidine kinases
638 that regulate initiation of sporulation in *Bacillus subtilis*. *Molecular cell* *13*, 689-701.
- 639 Saghatelian, A., and Couso, J.P. (2015). Discovery and characterization of smORF-encoded bioactive
640 polypeptides. *Nat Chem Biol* *11*, 909-916.
- 641 Samayoa, J., Yildiz, F.H., and Karplus, K. (2011). Identification of prokaryotic small proteins using a
642 comparative genomic approach. *Bioinformatics* *27*, 1765-1771.
- 643 Schaeffer, P., Millet, J., and Aubert, J.P. (1965). Catabolic repression of bacterial sporulation. *Proc*
644 *Natl Acad Sci U S A* *54*, 704-711.
- 645 Schmalisch, M., Maiques, E., Nikolov, L., Camp, A.H., Chevreux, B., Muffler, A., Rodriguez, S.,
646 Perkins, J., and Losick, R. (2010). Small genes under sporulation control in the *Bacillus subtilis*
647 genome. *J Bacteriol* *192*, 5402-5412.
- 648 Scholefield, G., and Murray, H. (2013). YabA and DnaD inhibit helix assembly of the DNA
649 replication initiation protein DnaA. *Mol Microbiol* *90*, 147-159.
- 650 Setlow, P. (2007). I will survive: DNA protection in bacterial spores. *Trends in microbiology* *15*,
651 172-180.
- 652 Skarstad, K., and Katayama, T. (2013). Regulating DNA replication in bacteria. *Cold Spring Harbor*
653 *perspectives in biology* *5*, a012922.
- 654 Slavoff, S.A., Heo, J., Budnik, B.A., Hanakahi, L.A., and Saghatelian, A. (2014). A human short
655 open reading frame (sORF)-encoded polypeptide that stimulates DNA end joining. *J Biol Chem* *289*,
656 10950-10957.

- 657 Slavoff, S.A., Mitchell, A.J., Schwaid, A.G., Cabili, M.N., Ma, J., Levin, J.Z., Karger, A.D., Budnik,
658 B.A., Rinn, J.L., and Saghatelian, A. (2013). Peptidomic discovery of short open reading frame-
659 encoded peptides in human cells. *Nat Chem Biol* 9, 59-64.
- 660 Soufo, C.D., Soufo, H.J., Noirot-Gros, M.F., Steindorf, A., Noirot, P., and Graumann, P.L. (2008).
661 Cell-cycle-dependent spatial sequestration of the DnaA replication initiator protein in *Bacillus*
662 *subtilis*. *Dev Cell* 15, 935-941.
- 663 Staudt, A.C., and Wenkel, S. (2011). Regulation of protein function by 'microProteins'. *EMBO*
664 *reports* 12, 35-42.
- 665 Sterlini, J.M., and Mandelstam, J. (1969). Commitment to sporulation in *Bacillus subtilis* and its
666 relationship to development of actinomycin resistance. *The Biochemical journal* 113, 29-37.
- 667 Storz, G., Wolf, Y.I., and Ramamurthi, K.S. (2014). Small proteins can no longer be ignored. *Annu*
668 *Rev Biochem* 83, 753-777.
- 669 Stragier, P., Bonamy, C., and Karmazyn-Campelli, C. (1988). Processing of a sporulation sigma
670 factor in *Bacillus subtilis*: how morphological structure could control gene expression. *Cell* 52, 697-
671 704.
- 672 Straub, D., and Wenkel, S. (2017). Cross-Species Genome-Wide Identification of Evolutionary
673 Conserved MicroProteins. *Genome biology and evolution* 9, 777-789.
- 674 Tanaka, K., Henry, C.S., Zinner, J.F., Jolivet, E., Cohoon, M.P., Xia, F., Bidnenko, V., Ehrlich, S.D.,
675 Stevens, R.L., and Noirot, P. (2013). Building the repertoire of dispensable chromosome regions in
676 *Bacillus subtilis* entails major refinement of cognate large-scale metabolic model. *Nucleic Acids Res*
677 41, 687-699.
- 678 VanOrsdel, C.E., Kelly, J.P., Burke, B.N., Lein, C.D., Oufiero, C.E., Sanchez, J.F., Wimmers, L.E.,
679 Hearn, D.J., Abuikhdair, F.J., Barnhart, K.R., *et al.* (2018). Identifying New Small Proteins in
680 *Escherichia coli*. *Proteomics* 18, e1700064.
- 681 Veening, J.W., Murray, H., and Errington, J. (2009). A mechanism for cell cycle regulation of
682 sporulation initiation in *Bacillus subtilis*. *Genes & development* 23, 1959-1970.
- 683 Westers, H., Dorenbos, R., van Dijl, J.M., Kabel, J., Flanagan, T., Devine, K.M., Jude, F., Seror, S.J.,
684 Beekman, A.C., Darmon, E., *et al.* (2003). Genome engineering reveals large dispensable regions in
685 *Bacillus subtilis*. *Mol Biol Evol* 20, 2076-2090.
- 686 Wu, L.J., and Errington, J. (2011). Nucleoid occlusion and bacterial cell division. *Nat Rev Microbiol*
687 10, 8-12.
- 688 Wu, W., and Jin, S. (2005). PtrB of *Pseudomonas aeruginosa* suppresses the type III secretion system
689 under the stress of DNA damage. *J Bacteriol* 187, 6058-6068.
- 690 Yang, X., Jensen, S.I., Wulff, T., Harrison, S.J., and Long, K.S. (2016). Identification and validation
691 of novel small proteins in *Pseudomonas putida*. *Environmental microbiology reports* 8, 966-974.
- 692 Zanet, J., Benrabah, E., Li, T., Pelissier-Monier, A., Chanut-Delalande, H., Ronsin, B., Bellen, H.J.,
693 Payre, F., and Plaza, S. (2015). Pri sORF peptides induce selective proteasome-mediated protein
694 processing. *Science* 349, 1356-1358.
- 695 Zuber, P. (2001). A peptide profile of the *Bacillus subtilis* genome. *Peptides* 22, 1555-1577.
- 696

697 10 Legends to figures

698 Figure 1

699 **A)** SknR transcriptionally repress the *yqaF-yqaN* operon of the skin element. **B-C) Yeast two hybrid**
700 **interaction assay.** Haploid yeast strains expressing *yqaH*, *dnaA* and *yabA* infusion with the BD and
701 AD domains of *gal4* are separately introduced into haploid yeast strains. Binary interactions are
702 tested by the ability of diploids to grow onto selective media. **D) DnaA interaction with YqaH and**
703 **regulators.** Numbers refer to amino acid boundaries (see also Figure S1). Schematic representation
704 of the architecture of the four functional domains of DnaA with associated functions as illustrated by
705 colors. The binding of negative regulators to their targeted DnaA functional domain is illustrated
706 accordingly. The YqaH interacting domains of DnaA with associated yeast 2HB interacting
707 phenotypes (IP) are indicated. (+ and -) refers growth or absence of growth on selective media,
708 reflecting interacting or loss of interaction phenotype, respectively.

709

710 Figure 2:

711 **YqaH triggers *dnaA*-related phenotypes. A) Effect of *yqaH* expression on growth.** Cells
712 carrying plasmids pDG148 (control, plain lines) or pDG148-*yqaH* (dashed lines) were examined in
713 the presence of IPTG (0.5 mM) over 5 hours. Growth was monitored either by OD600 (left x-axe,
714 black) or by cells viability, measured as the number of colony forming units per ml, normalized by
715 OD600 (right x-axe, red). **B) Nucleoid morphological defects.** Samples of living cells (OD or
716 time?) were examined by fluorescent microscopy after staining with of FM4-64 (membrane dye
717 false-colored in red) and DAPI (DNA dye, false-colored in blue). White and yellow arrows indicate
718 guillotined chromosomes resulting from septal closing over nucleoids and aberrant nucleoid
719 segregation patterns, respectively and typical example of chromosomal segregation defects is
720 magnified. Scale bares are 5 μm . **C) YqaH affects *dnaA* expression.** Cells harboring either the
721 pDG148 or pDG148-*yqaH* were grown in LB in the presence of IPTG. RNAs from exponentially
722 grown cells (OD600~0.3) were extracted and expression levels of the *dnaA* gene were monitored by
723 qPCR in the presence (+) or absence (-) of YqaH (*** P<0.001).

724

725 Figure 3:

726 **YqaH triggers sporulation and Spo0A-related phenotypes. A-B) YqaH expression inhibits**
727 **sporulation.** Cells carrying plasmids pDG148 (control) or pDG148-*yqaH* were grown in DSM
728 media in the presence of IPTG (0.5 mM) added at the onset (t_0) of sporulation. Sporulant cells were
729 observed at different time after initiation of sporulation. **A)** Snapshot captures of light and
730 fluorescence microscopy at indicated t_{hrs} time. Cells were stained with fluorescent membrane dye
731 FM4-64 (left panel). **B)** Sporulating cells were quantified by monitoring asymmetric septa, engulfed
732 forespore and free spores, in the presence (+) or absence (-) of YqaH. Ratio were determined from
733 observation of > 500 cells over 2 independent experiments and 3 biological replicates per
734 experiment. **C) YqaH affects expression Spo0A-regulated genes.** Cells harboring either the

735 pDG148 or pDG148-yqaH were grown in DSM. IPTG was. Expression levels of *spoIIE* and *spoIIGA*
736 genes from the Spo0A regulon were monitored by real-time qPCR in the presence (+) or absence (-)
737 of YqaH and expressed as relative expression ratio compared to control (-) (***) $P < 0.001$, $n \geq 6$).
738

739 **Figure 4:**

740 **Restoration of replication initiation defects by YqaH_DnaA LOI mutation.** Exponentially
741 growing *B. subtilis* cells carrying either pDG148 (-), pDG148-yqaH (WT), pDG148-yqaH LOI
742 mutant derivatives K17E or R56W were grown in the presence of IPTG and harvested at similar
743 OD₆₀₀~0.3 and assessed for various *dnaA*-related phenotypes: **(A) Nucleoid segregation and**
744 **morphology.** Cells were treated with DAPI to reveal nucleoids (false-colored blue) and with the
745 membrane dye FM4-64 (false colored red). **B-C-D) Analysis of DnaA-dependent replication**
746 **initiation phenotypes.** **B)** Ori:ter ratio; Origin-proximal and Terminus proximal DNA sequences
747 were quantified by qPCR. **C)** Visualization of origins foci in living cells. Origins are tagged through
748 binding of the GFP-lacI repressor to LacO operator sequences inserted at proximal location from
749 OriC. **D)** Averaged number of replication origins per cell determined as the number of LacI-GFP foci
750 upon induced condition in control (-), WT and K17E- mutant derivative of YqaH. Statistical
751 significance are illustrated by stars (t-test; . Ori:ter: $n=6$; *dnaA* mRNA: $n=12$; $P < 0.01$ *; $P < 0.001$ **).
752 **E) Effect of YqaH LOI mutant on dnaA expression.** Cells harboring either the pDG148, pDG148-
753 yqaHWT or K17E and R56W mutated derivatives were grown in LB in the presence of IPTG. RNAs
754 from exponentially grown cells (OD₆₀₀~0.3) were extracted and expression levels of the *dnaA* gene
755 were monitored by qPCR in the presence (+) or absence (-) of YqaH (*** $P < 0.001$).

756

757 **Figure 5:**

758 **Role of K17E DnaA_LOI substitution in sporulation and biofilm formation.** **A)** 168 and Tf8
759 strains carrying plasmids pDG148 (control) or pDG148-yqaH and K17E mutant were grown in DSM
760 media in the presence of IPTG (0.5 mM) added at the onset (t_0) of sporulation. Sporulant cells were
761 observed - hours after initiation of sporulation (as described in figure 3). **B)** Surface rendering of
762 biofilms pellicles of 168 strain expressing yqaH or yqaH-K17E mutant after 48h in Mgss media.
763 Biomass was averaged from 8 samples. Pairwise comparisons were performed using the Tukey
764 Method (* $p \leq 0.05$ ** $p \leq 0.01$ *** $p \leq 0.001$).

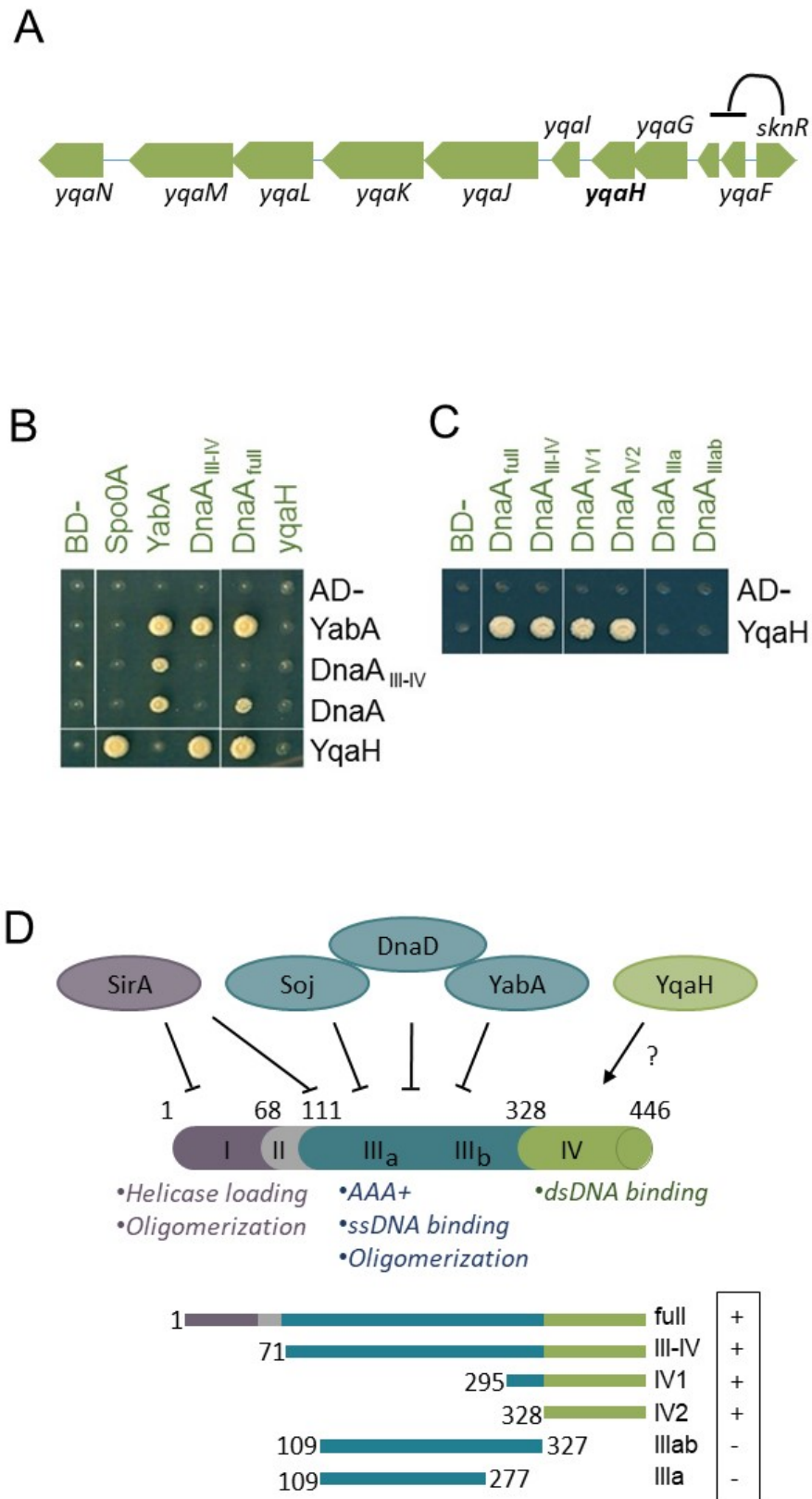
765 **Table 1:**

766 **YqaH_LOI mutational screen.** Aminoacid substitution affecting interaction with DnaA and/or
767 DnaN are indicated with their associated interaction phenotype. (-) refers as a total loss of interaction
768 phenotype leading to absence of growth on both -LUH and -LUA media. (+/-) refers as a partial loss
769 of interaction leading to some growth on the -LUH but not -LUA; see also Figure S1 for additional
770 explanation.

771

772 **Figure 1**

773

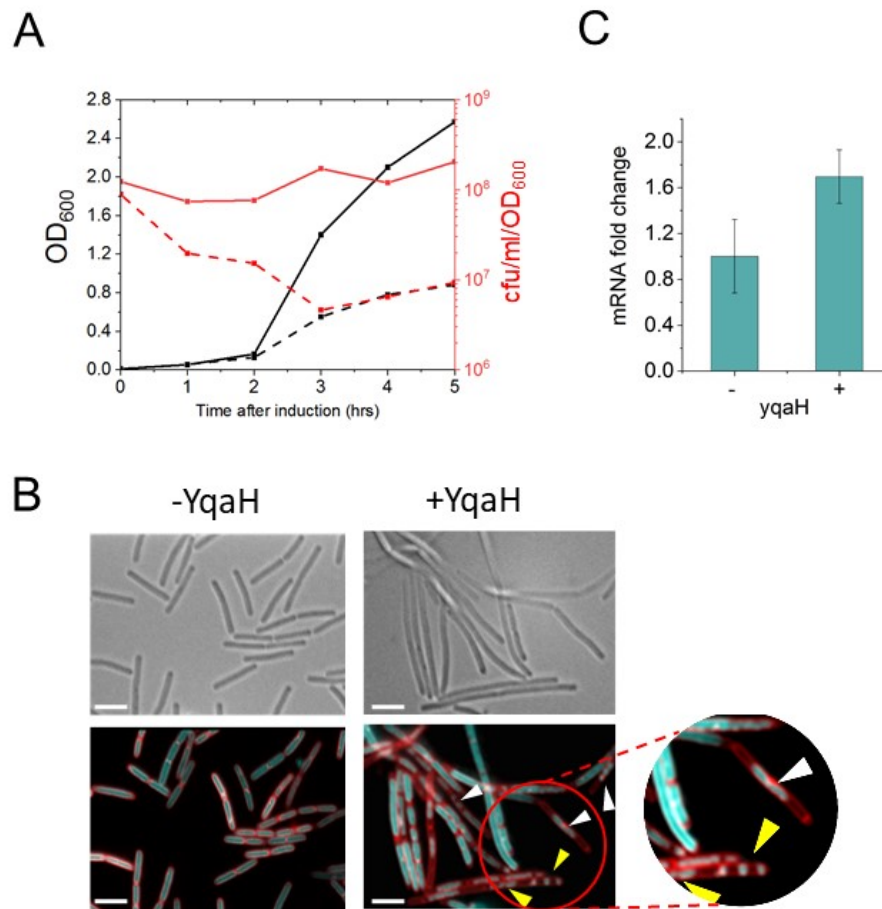


774 **Figure 2**

775

776

777



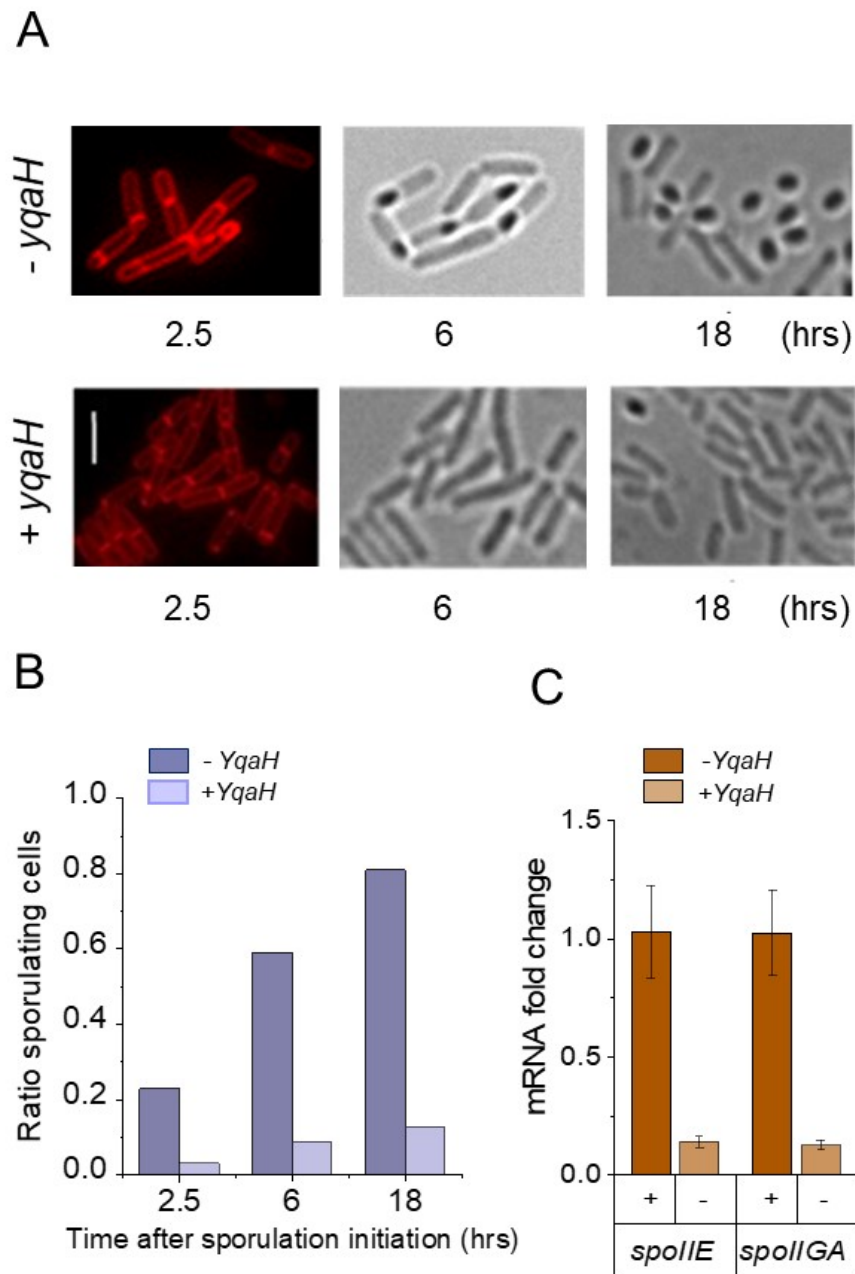
778 **Figure 3**

779

780

781

782



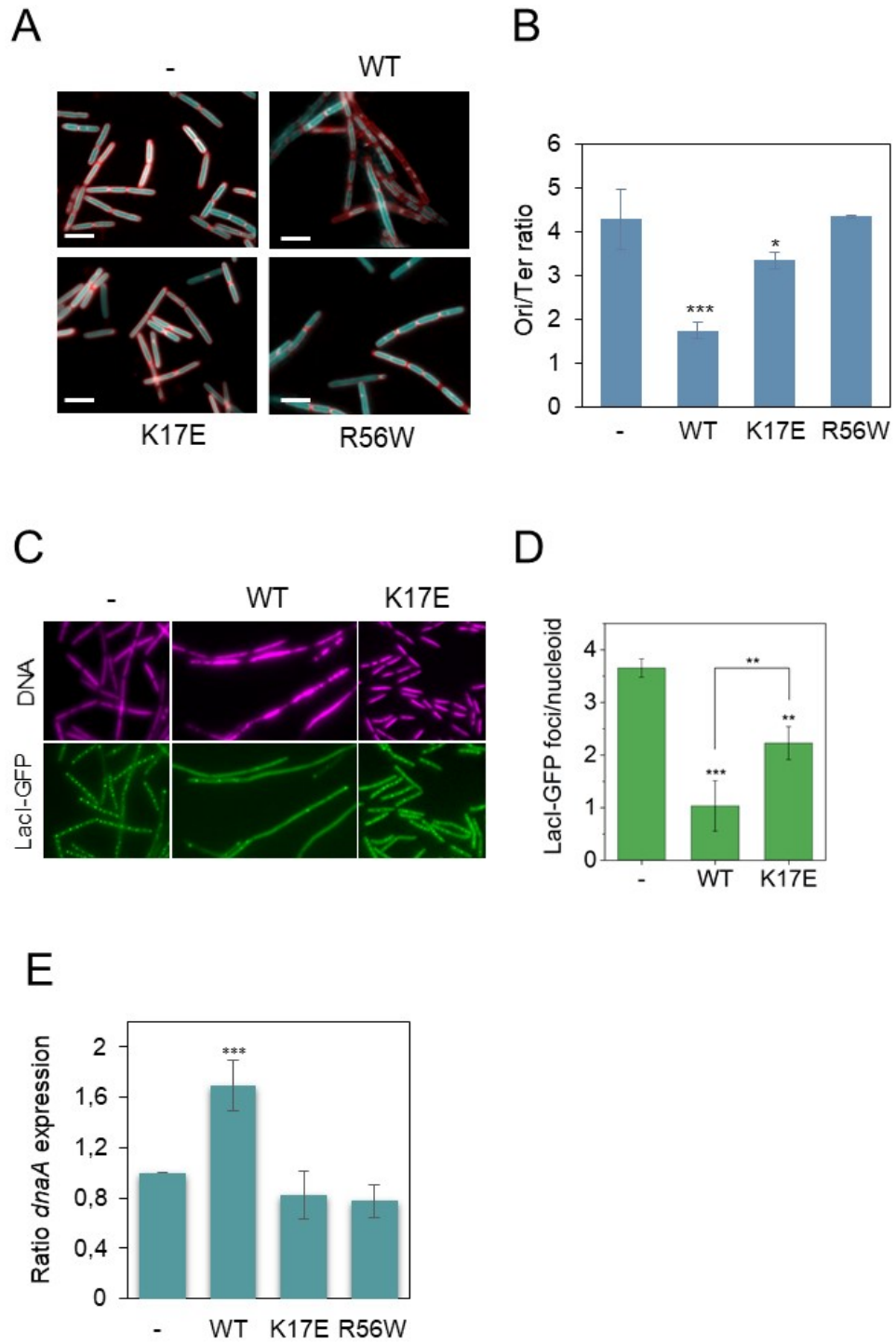
783 **Figure 4**

784

785

786

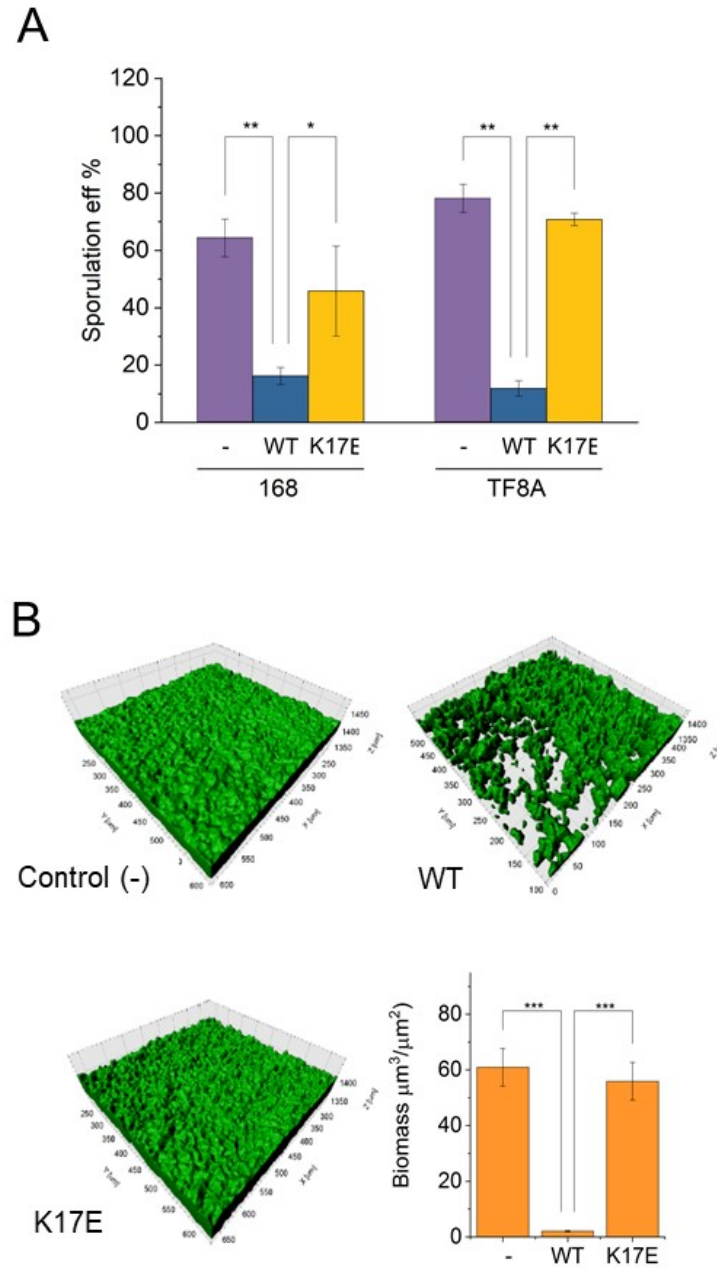
787



788 **Figure 5**

789

790



791 **Table 1**

792

		DnaA	Spo0A
YqaH_LOI	D10G	-	-
	R16G	+/-	+
	K17E	-	+
	S20L	-	-
	S25T	+/-	+/-
	M27T	+/-	+
	L28P	-	-
	Y37H	+/-	+
	E38K	-	+
	E38V	+/-	+
	A40T	+/-	+/-
	L43P	-	-
	A44V	+/-	+
	K48E	-	+
	R56W	-	+
L57P	-	-	

793

794

795

796

797